USGS
science for a changing world

Controls on the Physical Properties of Gas-Hydrate-Bearing Sediments Because of the Interaction Between Gas Hydrate and Porous Media

Scientific Investigations Report 2005-5143

U.S. Department of the Interior
U.S. Geological Survey

Controls on the Physical Properties of Gas-Hydrate-Bearing Sediments Because of the Interaction Between Gas Hydrate and Porous Media

By Myung W. Lee and Timothy S. Collett

Scientific Investigations Report 2005-5143

U.S. Department of the Interior
U.S. Geological Survey

U.S. Department of the Interior
Gale A. Norton, Secretary

U.S. Geological Survey
P. Patrick Leahy, Acting Director

U.S. Geological Survey, Reston, Virginia: 2005
Version 1.0
Posted online August 2005

This publication is *only* available online at URL:
http://pubs.usgs.gov/sir/2005/5143/

For information on other USGS products and ordering information:
World Wide Web: http://www.usgs.gov/pubprod/
Telephone: 1-888-ASK-USGS

For more information on the USGS—the Federal source for science about the Earth,
its natural and living resources, natural hazards, and the environment:
World Wide Web: http://www.usgs.gov/
Telephone: 1-888-ASK-USGS

Suggested citation:
Lee, M.W., and Collett, T.S., 2005, Controls on the physical properties of gas-hydrate-bearing sediments because of the interaction between gas hydrate and porous media: U.S. Geological Survey Scientific Investigations Report 2005-5143, 15 p.

Contents

Figures

Table

Controls on the Physical Properties of Gas-Hydrate-Bearing Sediments Because of the Interaction Between Gas Hydrate and Porous Media

By Myung W. Lee[1] and Timothy S. Collett[1]

Abstract

Physical properties of gas-hydrate-bearing sediments depend on the pore-scale interaction between gas hydrate and porous media as well as the amount of gas hydrate present. Well log measurements such as proton nuclear magnetic resonance (NMR) relaxation and electromagnetic propagation tool (EPT) techniques depend primarily on the bulk volume of gas hydrate in the pore space irrespective of the pore-scale interaction. However, elastic velocities or permeability depend on how gas hydrate is distributed in the pore space as well as the amount of gas hydrate. Gas-hydrate saturations estimated from NMR and EPT measurements are free of adjustable parameters; thus, the estimations are unbiased estimates of gas hydrate if the measurement is accurate. However, the amount of gas hydrate estimated from elastic velocities or electrical resistivities depends on many adjustable parameters and models related to the interaction of gas hydrate and porous media, so these estimates are model dependent and biased. NMR, EPT, elastic-wave velocity, electrical resistivity, and permeability measurements acquired in the Mallik 5L-38 well in the Mackenzie Delta, Canada, show that all of the well log evaluation techniques considered provide comparable gas-hydrate saturations in clean (low shale content) sandstone intervals with high gas-hydrate saturations. However, in shaly intervals, estimates from log measurement depending on the pore-scale interaction between gas hydrate and host sediments are higher than those estimates from measurements depending on the bulk volume of gas hydrate.

Introduction

Important questions for gas hydrate research are (1) Where do the gas hydrates occur? (2) How much gas hydrate is there? (3) Why do gas hydrates occur and how do gas hydrates occur in particular geological settings (Collett, 2002)? In order to answer " how much" and " how do hydrates occur in nature," various downhole well measurements have been used to analyze the occurrence of gas hydrate in various geological settings (Collett, 2002). Well logs have also been used to assess the pore-scale interaction between gas hydrate and host sediments (Kleinberg and others, 2003). The most commonly used methods of estimating gas-hydrate saturations are electrical resistivity (for example, Collett, 1998; Hyndman and others, 1999; Collett and Ladd, 2000) and acoustic logs (for example, Helgerud and others, 1999; Guerin and others, 1999; Lee and Collett; 1999). However, it is not fully understood to what degree gas hydrate increases sediment resistivity or velocity, which depends on how gas hydrate interacts with pore space.

Some of the recent measurements for gas-hydrate-bearing sediments depend only on the bulk volume of gas hydrate irrespective of the pore-scale interaction of gas hydrate. Density log measurements depend only on the bulk volume of constituents within a sediment sequence. The NMR log measures the total volume of water in the sediment (that is free water, capillary water, and bound water), and the EPT log measures the electromagnetic travel time in sediments and depends only on the bulk volume of constituent components. By combining density and the NMR or EPT log measurement, gas-hydrate saturations can be estimated (Kleinberg and others, 2003). Akihisa and others (2002) used the NMR porosity data to estimate in-situ gas-hydrate saturations in the Nankai trough MET1 2000 test well, offshore southeast Japan. Kleinberg and others (in press) used NMR and density measurements, and Sen and Goldberg (in press) used the EPT data to estimate gas-hydrate saturations at the Mallik 5L-38 well, Mackenzie Delta, N.W.T., Canada.

Elastic velocities of gas-hydrate-bearing sediments depend on how the gas hydrate is distributed at the pore scale as well as the amount of gas hydrate. Helgerud (2001) presented four different pore-scale hydrate distribution models: (a) hydrate floating in the pore fluid, (b) hydrate as a load-bearing member of the matrix, (c) hydrate cementing grain contacts and evenly coating grains, and (d) hydrate acting as a cement and forming only at grain contacts. Elastic velocities increase dramatically at low gas-hydrate saturations because gas hydrate behaves as a floating constituent in the pore fluid to cementing grain contacts. Electrical resistivity and permeability depend on the tortuosity of sediments, which is related to how gas hydrate is distributed in the sediment pore as well as the amount of gas hydrate.

[1]U.S. Geological Survey, Box 25046, Mail Stop 939, Denver Federal Center, Denver, Colorado 80225. e-mail: mlee@usgs.gov.

Because gas-hydrate saturation estimates from NMR and EPT well log measurements depend only on the bulk volume of gas hydrate and are independent of the pore-scale interaction of gas hydrate with pore space, NMR and EPT data can be used to establish the baseline necessary to infer the pore-scale interaction for elastic velocities or permeability. Kleinberg and others (2003) preferred a pore-filling model to the cementation model based on permeability measured by an NMR tool. Based on elastic velocities and amplitude versus offset analysis, Ecker and others (1998) and Lee and Collett (2001a) supported the pore-filling model for the occurrence of gas hydrate. However, Guerin and others (1999) prefer the cementation model (grain coating) based on the well log analysis at Blake Ridge.

This paper presents the result of analyzing density, NMR, EPT, gamma ray, *P*-wave velocity, *S*-wave velocity, resistivity, and permeability logs acquired in the Mallik 5L-38 well, Mackenzie Delta, N.W.T., Canada, in order to examine the accuracy of each estimation method and to infer the interaction between gas hydrate and porous media. The gas-hydrate saturations from NMR and EPT measurements are compared to those from elastic velocities and resistivities, and discrepancies among various estimations are discussed.

Theoretical Background

Downhole well logging tools can be used to measure physical properties of gas-hydrate-bearing sediments. Some measurements such as density and NMR porosity depend only on the bulk volume of gas hydrate in the pore space. However, other measurements, such as elastic velocities and permeability, depend on pore-scale interactions between gas hydrate and porous media as well as the bulk volume of gas hydrate.

Log Measurements Controlled Only by Gas-Hydrate Content

Density

The bulk density of gas-hydrate-bearing sediment (ρ_b) can be written as

$$\rho_b = \rho_{ma}(1-\phi) + \rho_f\phi(1-S) + \rho_h\phi S \tag{1}$$

where

ϕ is the total porosity,

ρ_{ma}, ρ_f, and ρ_h are density of matrix, density of fluid, and density of gas hydrate, respectively, and

S is the gas-hydrate saturation in the pore space.

NMR

The NMR porosity (ϕ_{NMR}) measures the pore space occupied only by water (bound, capillary, and free water) and is given by the following equation

$$\phi_{NMR} = \phi(1-S) \tag{2}$$

From equations 1 and 2

$$\phi = \frac{\phi_D + \lambda_h\phi_{NMR}}{1+\lambda_h} \tag{3}$$

$$S = \frac{\phi - \phi_{NMR}}{\phi} \tag{4}$$

where

$$\lambda_h = \frac{\rho_f - \rho_h}{\rho_{ma} - \rho_f} \quad \text{and} \quad \phi_D = \frac{\rho_{ma} - \rho_b}{\rho_{ma} - \rho_f} \tag{5}$$

Note that ϕ_D is the conventional density porosity derived using a two-component system (matrix and water) and ϕ_{NMR} is the same as the water-filled porosity defined in Lee and Collett (2001a), which is $\phi_w = (1 - S)\phi$. Porosity given in equation 3 is total porosity, which is the space occupied by water and gas hydrate in the pore space. Total porosity and porosity are used interchangeably in this paper.

EPT

For the EPT measurement, the dielectric permittivity can be written as

$$\sqrt{\varepsilon_r} = (1-\phi)\sqrt{\varepsilon_{rm}} + \phi S\sqrt{\varepsilon_{rh}} + \phi(1-S)\sqrt{\varepsilon_{rw}} \tag{6}$$

where

ε_r, ε_{rm}, ε_{rw}, and ε_{rh} are relative permittivity of sediments, matrix, water, and gas hydrate, respectively (Sun and Goldberg, in press).

From equation 6, the gas-hydrate saturation can be written as

$$S = \frac{\sqrt{\varepsilon_r} - (1-\phi)\sqrt{\varepsilon_{rm}} - \phi\sqrt{\varepsilon_{rw}}}{\phi\left(\sqrt{\varepsilon_{rh}} - \sqrt{\varepsilon_{rw}}\right)} \tag{7}$$

Propagation velocity is related to the dielectric permittivity as

$$\varepsilon_r = c^2\left(t_{pl}^2 - \frac{\alpha^2}{3604}\right) \tag{8}$$

where

c is the speed of light in vacuum,

t_{pl} is the slowness or propagation time of the sediments, and

α is attenuation.

If we assume that $t_{pl} >> \alpha / \sqrt{3604}$, then equation 7 can be written as

$$S = \frac{t_{pm} - t_{pw}}{t_{ph} - t_{pw}} + \frac{t_{pl} - t_{pm}}{\phi(t_{ph} - t_{pw})} \tag{9a}$$

where

t_{pm}, t_{ph}, and t_{pw} are the propagation time through the matrix, gas hydrate, and water, respectively.

If we further assume that t_{ph} is the same as t_{pm}, then

$$S = 1 + \frac{t_{pl} - t_{pm}}{\phi(t_{pm} - t_{pw})} \tag{9b}$$

Note that Sun and Goldberg (in press) used equation 7 and Kleinberg and others (in press) used equation 9b to estimate gas-hydrate saturations from the EPT measurements.

If we define ϕ_{EPT} as follows

$$\phi_{EPT} = \frac{t_{pm} - t_{pl}}{t_{pm} - t_{pw}} \tag{10}$$

then, equation 9b can be written as

$$S = \frac{\phi - \phi_{EPT}}{\phi} \tag{11}$$

This is an identical form as the equation shown in equation 4, and ϕ_{EPT} is identical to the water-filled porosity defined in Lee and Collett (2001a).

Simultaneous Estimation of Porosity and Gas-Hydrate Saturations Using Density, NMR, and EPT Logs

Simultaneous estimation of porosity and gas-hydrate saturations using density, NMR, and EPT measurements for gas-hydrate-bearing sediments can be derived as follows

$$\phi(\rho_{ma} - \rho_f) + \phi S(\rho_f - \rho_h) = \rho_{ma} - \rho_b \tag{12a}$$

$$\phi - \phi S = \phi_{NMR} \tag{12b}$$

$$\phi(\sqrt{\varepsilon_{rw}} - \sqrt{\varepsilon_{rm}}) + \phi S(\sqrt{\varepsilon_{rh}} - \sqrt{\varepsilon_{rw}}) = \sqrt{\varepsilon_r} - \sqrt{\varepsilon_{rm}} \tag{12c}$$

Equation 12 can be written in the following matrix form by defining $V_h = \phi S$,

$$\begin{bmatrix} \rho_{ma} - \rho_f & \rho_f - \rho_h \\ 1 & -1 \\ \sqrt{\varepsilon_{rw}} - \sqrt{\varepsilon_{rm}} & \sqrt{\varepsilon_{rh}} - \sqrt{\varepsilon_{rw}} \end{bmatrix} \begin{bmatrix} \phi \\ V_h \end{bmatrix} = \begin{bmatrix} \rho_{ma} - \rho_b \\ \phi_{NMR} \\ \sqrt{\varepsilon_r} - \sqrt{\varepsilon_{rm}} \end{bmatrix} \tag{13}$$

Note that equation 12c, suggested by Sun and Goldberg (in press) for the EPT, is used for the inversion in equation 13. Using the generalized inverse, the parameter matrix $(\phi, V_h)^T$ can be calculated.

In the case that equation 9b by Kleinberg and others (in press) is used for the EPT, the matrix equation is in the following form

$$\begin{bmatrix} \rho_{ma} - \rho_f & \rho_f - \rho_h \\ 1 & -1 \\ 1 & -1 \end{bmatrix} \begin{bmatrix} \phi \\ V_h \end{bmatrix} = \begin{bmatrix} \rho_{ma} - \rho_b \\ \phi_{NMR} \\ \phi_{EPT} \end{bmatrix} \tag{14}$$

Log Measurements Controlled by Pore-Scale Interaction

The elastic velocities, electrical resistivity, and permeability of gas-hydrate-bearing sediments depend not only on the amounts of gas hydrate in the pore space but also on how the gas hydrate is distributed in the pore space. Whether gas hydrates fill the pore space (pore-filling model) or cement the grains (cementation model) is controversial because laboratory and in situ observations yield different interpretations of pore-scale interactions of gas hydrates (Kleinberg and others, 2003). Elastic velocities and permeability strongly depend on the mode of hydrate growth in pore space.

Velocity

Elastic velocities for the pore-filling model are derived from the modified Biot-Gassmann theory by Lee, or BGTL (Lee, 2002a, 2005), and velocities for the cementation model are derived from Dvorkin and Nur (1996), assuming that gas hydrate coats grains uniformly. In order to model gas hydrate as pore-filling material, the moduli of matrix (quartz, clay, and gas hydrate) are calculated using Hill's averaging formula (Hill, 1952), as shown in Helgerud and others (1999) and Lee (2002a).

Resistivity

The resistivity of water-saturated sediment can be expressed by the Archie relation (Archie, 1942) and is given by

$$R_t = \frac{aR_w}{\phi^m} \tag{15}$$

where

R_t is the resistivity of formation,

R_w is the resistivity of connate water, and

a and m are Archie parameters.

Theoretically, a should be 1, but analyses of measured data shows a different from 1 and the Humble relationship (Winsauer and others, 1952) uses $a = 0.62$. However, this is not a serious deficiency as long as the relation between porosity and resistivity is sufficiently accurate over the range of interest (Hearst and others, 2000). The cementation exponent m depends on the state of consolidation and appears to be entirely dependent upon particle shape for unconsolidated sediments. For this study, the Humble equation is used, that is $a = 0.62$ and $m = 2.15$ (Winsauer and others, 1952).

Gas-hydrate saturations can be estimated from the resistivity using the following equation

$$S = 1 - \left\{ \frac{aR_w}{R_t \phi^m} \right\}^{1/l} \tag{16}$$

where

l is an exponent depending on lithology and usually is taken as 1.9386 (Pearson and others, 1983).

Note that the porosity shown in equation 16 is total porosity.

Because NMR porosity measures space occupied only by water and is equal to the water-filled porosity, S is equal to zero if NMR or EPT porosity is used in equation 16. Therefore, the resistivity of pore fluid can be calculated as

$$R_w = \frac{R_t \phi_{NMR}^m}{a} \tag{17}$$

Permeability

A widely used starting point of permeability (k) of granular media is the Kozeny family of equations (Hearst and others, 2000). In terms of the ratio of pore surface to grain volume, permeability can be written as

$$k = \frac{\phi_{NMR}^3}{f\tau(1-\phi_{NMR})^2 (A/V)_{grain}^2} \tag{18}$$

where

f is a shape factor, which is on the order of unity,

τ is the tortuosity and given by $\tau = (L_a / L)^2$ where L_a is the path length for flow and L is the straight line distance associated with the pressure drop,

A is the internal surface area of the pore space, and

V is the grain volume.

The tortuosity and $(A/V)_{grain}^2$ depend on how the gas hydrate grows in the pore space.

The tortuosity and the formation factor (F), which is $F = R_t / R_w$, is related by (Walsh and Brace, 1984)

$$\tau = F\phi_{NMR} = \frac{a}{\phi_{NMR}^{m-1}} \tag{19}$$

Using the formation factor, permeability shown in equation 19 can be written as

$$k = \frac{R_h^2}{fF} \tag{20}$$

with

$$R_h = \frac{\phi_{NMR}}{(1-\phi_{NMR})(A/V)_{grain}}$$

Permeability is inversely proportional to electrical resistivity. Therefore, the pore-scale interaction between gas hydrate and porous media similarly affects both permeability and electrical resistivity.

Joint Inversion of Acoustic and Resistivity Data

In order to estimate the gas-hydrate saturations and the electrical resistivity of pore water, a joint inversion of acoustic and resistivity was proposed by Lee (2002b). Let us define column vectors O and T as follows:

O = column vector of the velocities of P-wave (V_p), and S-wave (V_s), and the resistivity (R_t).

T = column vector of the computed or theoretical velocity of P-wave, velocity of S-wave, and resistivity.

Elastic velocities and resistivities can be approximated by the following equation

$$T(p^{n+1}) = T(p^n) + (\frac{\partial T}{\partial S})_n \Delta S + (\frac{\partial T}{\partial R_w})_n \Delta R_w + \ldots$$

or

$$\begin{bmatrix} V_p(p^{n+1}) \\ V_s(p^{n+1}) \\ R_t(p^{n+1}) \end{bmatrix} = \begin{bmatrix} V_p(p^n) \\ V_s(p^n) \\ R_t(p^n) \end{bmatrix} + \begin{bmatrix} \partial V_p(p^n)/\partial S, & \gamma \\ \partial V_s(p^n)/\partial S, & \gamma \\ \partial R_t(p^n)/\partial S, & \partial R_t(p^n)/\partial R_w \end{bmatrix} \begin{bmatrix} \Delta S \\ \Delta R_w \end{bmatrix}$$

or

$$T(p^{n+1}) = T(p^n) + G\Delta p \tag{21}$$

where

p is a parameter vector consisting of S and R_w,

G is a 3×2 Jacobian matrix,

$\Delta S = S^{n+1} - S^n$,

$\Delta R_w = R_w^{n+1} - R_w^n$, and

$\Delta p = p^{n+1} - p^n$.

In the original inverse formulation, $\gamma = 0$ because R_w is only related to the electrical resistivity, not elastic velocities. This implies that the velocity equation is decoupled from the electrical resistivity equation. As explained in Lee (2002b), a coupling constant, γ, is introduced in an ad hoc way where the element of Jacobian matrix is zero in order to estimate R_w. Equation 21 can be solved for Δp using a generalized inverse.

Well Log Analysis

For this study, well logs acquired at the Mallik 5L-38, gas hydrate research well drilled at the Mackenzie Delta, N.W.T., Canada, are analyzed. The well logs used are bulk density, NMR porosity, EPT, gamma ray, *P*- and *S*-wave velocities, resistivity, and permeability from NMR.

The surficial sediments of the Mackenzie Delta are composed of modern deltaic sediments and older fluvial and glacial deposits. At depth, the area is underlain by deltaic sandstone and shales of Mesozoic and Cenozoic age that thicken to more than 12 km over a short distance seaward from the present shoreline. This sedimentary section overlies faulted Paleozoic rocks (Dallimore and Collett, 1997), and the Mallik 5L-38 well site overlies a large regional anticlinal structure. The sediments at this well site are unconsolidated, and the dominant clay type is illite.

NMR and EPT

The gas-hydrate saturations estimated from the NMR using equations 3 and 4 and from the EPT using equations 3 and 7, or the Sun and Goldberg (in press) approach using parameters in table 1, are shown in figure 1*A*. The depth range for figure 1 is from 843 to 1,161 m, where the hydrate-bearing interval is from 891 to 1,109 m (Lewis and Collett, in press). Gas-hydrate saturations estimated from the NMR logs in the Mallik 5L-38 well are higher than those estimated from the EPT. Note that the differences between NMR and EPT estimates are greater at lower saturations.

In the case that there is no gas hydrate in the pore, the NMR and EPT porosities should be equal to total porosity. Therefore, we should see a large numbers of near-zero saturations in figure 1 because the depth intervals used for figure 1 include non-gas-hydrated intervals. However, figure 1*A* indicates that the EPT method greatly underestimates gas-hydrate saturations. Even though gas-hydrate saturations estimated from the NMR appear to be more accurate than those from the EPT log measurements, the NMR data from the Mallik 5L-38 well appear to underestimate the gas-hydrate content at low gas-hydrate saturations.

Figure 1*B* shows estimated gas-hydrate saturations using the Kleinberg and others (in press) approach for the EPT. Overall, estimates from the NMR are lower than those from the EPT. However, gas-hydrate saturations estimated from the EPT using Kleinberg and others' approach agree better with those from the NMR measurement. Although equations used by Kleinberg and others (in press) are an approximation of equations used by Sun and Goldberg (in press), they perform better than the exact equations, suggesting that some of the assumed parameters shown in table 1 are not accurate for the EPT measurement at this well site.

Figure 1*C* shows estimated gas-hydrate saturations from the joint inversion of NMR and EPT using equation 14, or the NE-inversion. Estimates from the NE-inversion agree better with those from the NMR. However, scattering near $S = 0$ percent suggests that either EPT- or NMR-derived saturations from the Mallik 5L-38 well are not accurate at low gas-hydrate saturations.

Velocity and Resistivity

Gas-hydrate saturations estimated from the *P*-wave velocity, *S*-wave velocity, and formation resistivity using equation 21, or the PSR-inversion, are shown in figure 2 as a solid line. For comparison, estimates using equation 14, or NE-inversion, are shown as a dotted line in figure 2. The average saturation from the PSR-inversion technique is 0.25±0.29, whereas that calculated from the NE-inversion is 0.16±0.36. As shown in figure 2, for gas-hydrate saturations above 40 percent, the

Table 1. Electromagnetic propagation tool (EPT) parameters.

[SL, Sloan (1998); SG, Sun and Goldberg (in press); KFC, Kleinberg, Flaum, and Collett (in press)]

Definition	Symbol used	Value	Reference
Density of gas hydrate	ρ_h	0.91	SL
Relative dielectric permittivity of water	ε_{rw}	81	SG
Relative dielectric permittivity of gas hydrate	ε_{rh}	3	SG
Relative dielectric permittivity of matrix	ε_{rm}	5	SG
Propagation time through matrix (ns/m)	T_{pm}	6	KFC
Propagation time through water (ns/m)	T_{pw}	46	KFC

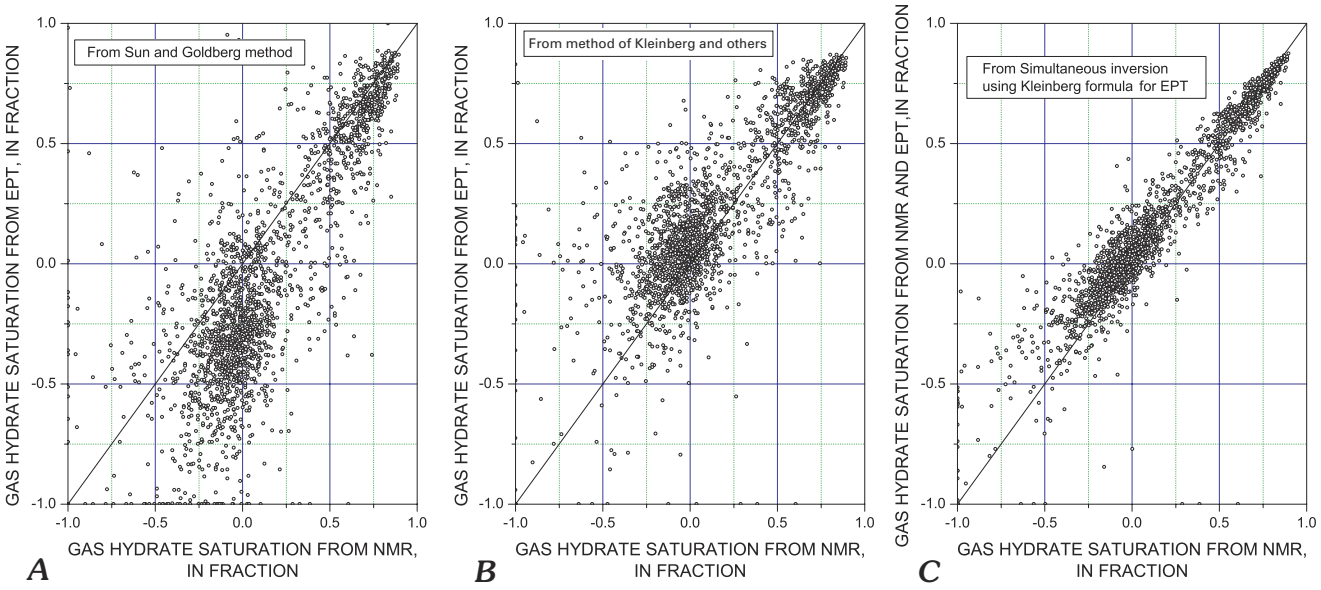

Figure 1. Gas-hydrate saturations estimated from nuclear magnetic resonance (NMR) and electromagnetic propagation tool (EPT) logs. *A*, Cross plot of gas-hydrate saturations estimated from NMR log and those from EPT based on Sun and Goldberg (in press). *B*, Cross plot of gas-hydrate saturations estimated from NMR log and those from EPT based on Kleinberg and others (in press). *C*, Cross plot of gas-hydrate saturations estimated from NMR log, and those from simultaneous inversion of NMR and EPT based on Kleinberg and others (in press).

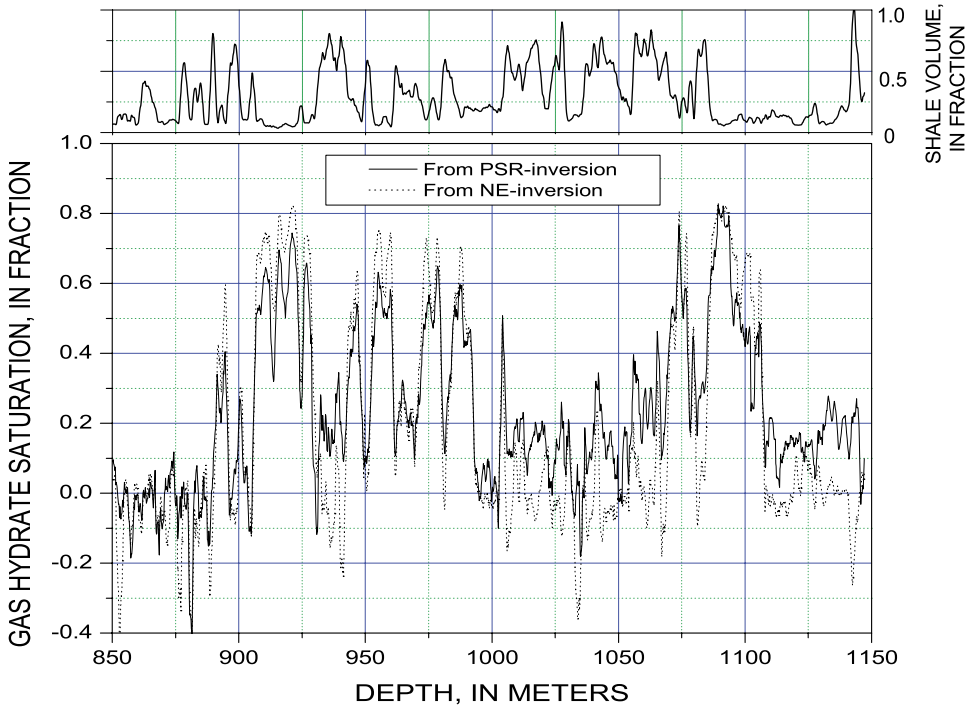

Figure 2. Gas-hydrate saturations estimated from NE-inversion method (using density, NMR, and EPT logs) shown as a dotted line, and those from PSR-inversion (using density, *P*-wave velocity, *S*-wave velocity, and resistivity) shown as a solid line. Shale volumes indicated on the top of figure. Estimates are 11-point running average (sampling interval ≈ 0.15 m). Note that gas-hydrate stability zone is between 891 and 1,109 m depth. NMR, nuclear magnetic resonance; EPT, electromagnetic propagation tool.

NE-inversion-derived saturations are higher than those from the PSR-inversion. However, the average saturation estimated from the NE-inversion is much lower than that from the PSR-inversion. This implies that, for low saturations of gas hydrate, the NMR or EPT may overestimate porosities or the PSR-inversion overestimates gas-hydrate saturations.

The result of the PSR-inversion for depths below 1,109 m (the non-gas-hydrate-bearing interval) indicates that there is some gas hydrate, an average of about 20 percent, which must be an error, and the result of the NE-inversion should be more accurate. Comparing estimates from the NE-inversion, the PSR-inversion technique appears to overestimate gas-hydrate saturations when gas-hydrate saturations are below about 20 percent, whereas the PSR-inversion method underestimates gas-hydrate saturations when saturations are above about 40 percent. The accuracy of saturations derived from the NE-inversion and the PSR-inversion will be discussed later.

Porosity and Permeability

Permeability can be calculated from the NMR measurement using the Keynon relation (Kenyon, 1992). Sediment permeability depends primarily on water-filled porosity, and their relationship is shown in figure 3. In figure 3, the well log measurements within the gas-hydrate stability zone at the Mallik 5L-38 well are classified into three groups depending on the gas-hydrate saturations estimated from the PS-inversion (using *P*- and *S*-wave velocities). For comparison, calculated permeability using an empirical relationship by Sen and others (1990) is plotted as solid and dotted lines with various NMR decay times, T_1.

Figure 3*A* shows the relationship between permeability and water-filled porosity calculated from the PS-inversion. For high gas-hydrate saturations (above 40 percent), the majority of data follows the relationship with T_1 = 25 ms (between T_1 = 50 and T_1 = 12.5); also, the majority of low gas-hydrate saturations follow the relationship with T_1 near 25 ms.

Figure 3*B* shows the relationship between permeability and water-filled porosity calculated from the NE-inversion. For high gas-hydrate saturations (above 40 percent), data primarily follow the relationship with T_1 = 50 ms, but the majority of low gas-hydrate saturations (less than 40 percent) follow the relationship with T_1 = 12.5 ms. Although the average porosity of high saturations is lower than that of lower saturations, the permeability predicted with a lower T_1 fits better for low gas-hydrate saturations.

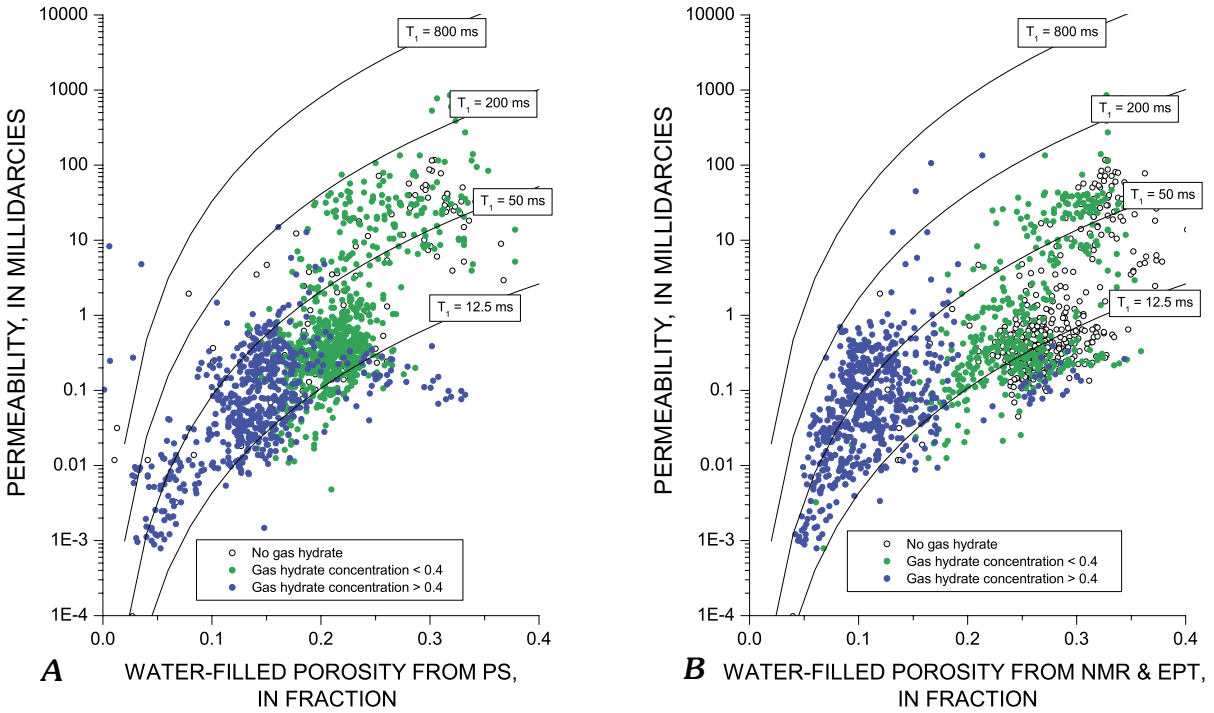

Figure 3. Relationship between permeability and water-filled porosity for samples within gas-hydrate stability zone (891–1,109 m). Measurements are classified into three groups based on gas-hydrate saturations. *A*, Water-filled porosity calculated from PS-inversion (*P*- and *S*-wave velocity). *B*, Water-filled porosity calculated from NE-inversion (NMR and EPT). Solid lines represent predicted permeabilities from the empirical relationship by Sen and others (1990). NMR, nuclear magnetic resonance; EPT, electromagnetic propagation tool.

Analysis and Results

Comparison among NE-inversion, PS-inversion, and Velocity Models

The gas-hydrate saturations or water-filled porosities estimated from NMR and EPT logs in the Mallik 5L-38 well are different from those from the PS-inversion. As mentioned previously, at high gas-hydrate saturations, saturations derived from the NMR or EPT logs are generally higher than those derived from velocity measurements. But at low saturations, the opposite is true. Because the general trend of well-log-derived gas-hydrate saturations are inversely proportional to the clay content in sediments, to a first order approximation, gas-hydrate saturations are inversely proportional to clay content in sediments, and the difference between results from the NE-inversion and PS-inversion could depend on the clay content of the logged sediments.

In order to reduce the variability in the log-derived gas-hydrate saturations due to porosity and clay-content differences, a subset of well log measurements at the Mallik 5L-38 well—in zones with clay volume contents less than 10 percent (average clay volume content of 7 percent) and total porosity between 34 percent and 36 percent—was analyzed and plotted in figure 4. Figure 4*A* shows *P*- and *S*-wave velocities with respect to the water-filled porosity calculated from the PS-inversion. Because gas-hydrate saturations are estimated from BGTL, the measured velocities with respect to the water-filled porosity calculated from the PS-inversion agree well with predicted velocities. However, cementation theory significantly overestimates velocities at low and medium saturations.

Figure 4*B* shows the result using water-filled porosity calculated from the NE-inversion. Because the water-filled porosity from the NE-inversion is independent of the velocity model, it serves as an independent measurement to check the validity of velocity models. At low water-filled porosities (or high gas-hydrate saturations), porosities estimated from the NE-inversion are a little lower than those estimated from the PS-inversion but generally agree with the predictions of the pore-filling model. At high water-filled porosities (or low gas-hydrate saturations), the majority of velocities are above the baseline velocities, which implies that the sediments contain no gas hydrate. Even though porosities estimated from the PS-inversion differ slightly from those estimated from the NE-inversion, the pore-filling model agrees better with the measurement than does the cementation theory.

Figure 5 shows an analysis similar to that discussed above considering relative permeabilities. Relative permeability is defined as the ratio of permeability of gas-hydrate-bear-

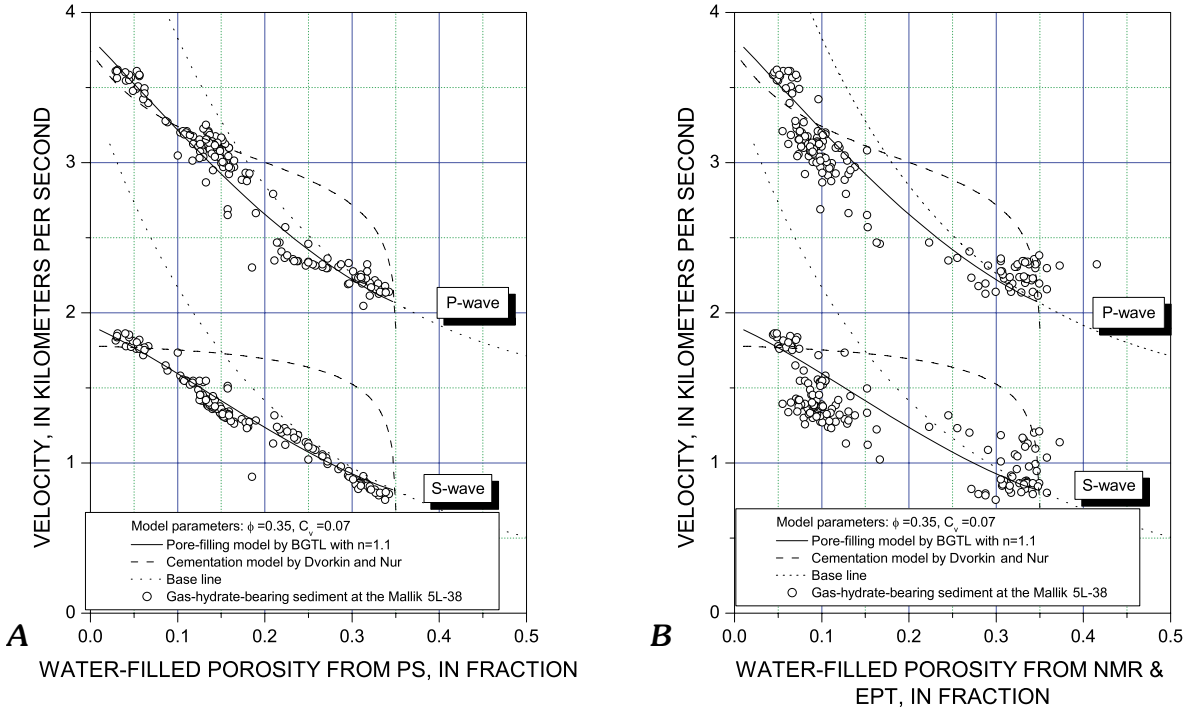

Figure 4. Relationship between velocities and water-filled porosity for samples having $0.34 < \phi < 0.36$ and $0 < C_v < 0.1$. Predicted velocities using the modified Biot-Gassmann theory by Lee (BGTL) shown as solid lines for gas-hydrate-bearing sediments having porosity of 0.35 and clay volume content of 0.07 with $n = 1.1$; predicted velocities shown as dashed lines using the cementation theory by Dvorkin and Nur (1996); predicted velocities shown as dotted lines for baseline velocity. *A*, Water-filled porosities calculated from PS-inversion. *B*, Water-filled porosities calculated from NE-inversion (NMR and EPT). *n*, BGTL parameter; ϕ, porosity in fraction; C_v, clay volume content in fraction; NMR, nuclear magnetic resonance; EPT, electromagnetic propagation tool.

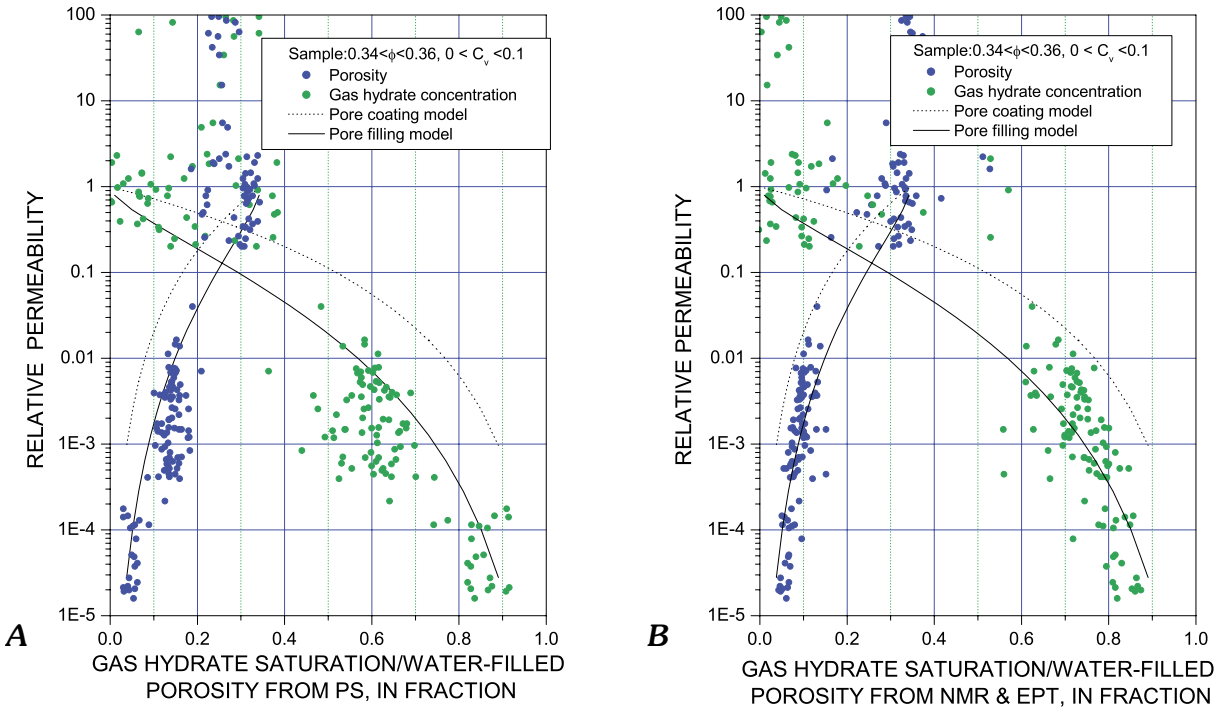

Figure 5. Relationship between permeability and water-filled porosity and gas-hydrate saturations for samples having 0.34 < ϕ < 0.36 and 0 < C_v < 0.1. Predicted permeabilities of gas-hydrate-bearing sediment using the pore-filling model shown as solid lines and as dotted lines for cementation model. *A*, Water-filled porosities and gas-hydrate saturations calculated from PS-inversion. *B*, Water-filled porosities and gas-hydrate saturations calculated from NE-inversion (NMR and EPT). ϕ, porosity in fraction; C_v, clay volume content in fraction; NMR, nuclear magnetic resonance; EPT, electromagnetic propagation tool.

ing sediment to the permeability of the same sediment without gas hydrate. For comparison, theoretical relative permeability of pore-coating and pore-filling models from Kleinberg and others (2003) are denoted in figure 5 as dotted and solid lines, respectively. Overall, the measured relative permeabilities with respect to gas-hydrate saturations estimated from the PS-inversion decreases faster than that predicted from the pore-filling model and decreases much faster than that from the pore-coating or cementation model. However, the rate of decrease of relative permeability with respect to gas-hydrate saturation from the NE-inversion is very similar to the prediction by the pore-filling model. The relationship between permeability and water-filled porosities (or gas-hydrate saturations) estimated from the PS-inversion and NE-inversion methods indicate that the pore-filling model is more accurate than the pore-coating model.

Previous discussions indicate that a pore-filling model of gas hydrate is preferable. However, it is difficult to determine whether PS-inversion based on the pore-filling model yields more accurate gas-hydrate saturations than the NE-inversion. Figure 5 suggests that the water-filled porosities derived from the NE-inversion appear to agree better with predictions of the pore-filling model, so gas-hydrate-saturation estimates from the NE-inversion would be more accurate. However, the pore-filling model proposed by Kleinberg and others (2003) does not account for the effect of blocking pore throats with gas-hydrate accumulations until very high saturations. Therefore, if a small amount of gas hydrate blocks some small pore throats, the predicted permeability from the pore-filling model would decrease more rapidly than is indicated in figure 5.

Comparison of Permeability with Other Empirical Equation

Nelson (1994) reviewed permeability-porosity relationships in sedimentary rocks. He summarized sand-pack models (Krumbein and Monk, 1943), grain-based models (Berg, 1970), surface-area models (Timur, 1968; Sen and others, 1990), and a pore-size model (Katz and Thompson, 1986). Among these empirical relations, Sen and others (1990) utilized proton NMR decay time, T_1, and derived the following empirical equation

$$k = 0.794(\phi^m T_1)^{2.15} \quad (22)$$

Equation 18 indicates that permeability depends on the $(V/A)^2_{grain}$. The proton decay in NMR is dominated by the presence of grain surface and $T_1 \propto (V/A)^{0.9}_{grain}$ (Sen and others, 1990). Therefore, the empirical relation shown in equation 22 is a reasonable approximation between porosity and permeability based on the theoretical relationship shown in equation 18.

Figure 6 shows results similar to those shown on figure 3 with a different classification using clay volume contents instead of gas-hydrate saturations. Figure 6 demonstrates that the permeability of clean sandstones measured by Doyen and others (1988) agrees well with equation 22 with T_1 = 800 ms. However, the permeability of clay-bearing sandstones measured by Sen and others (1990) matches permeability with T_1 = 800 ms near a porosity of 20 percent and decreases rapidly with decreasing porosity and matches T_1 = 25 ms near a porosity of 5 percent, implying a complicated effect of clay content on permeability.

Permeability with respect to water-filled porosity derived from PS-inversion follows predicted permeability with T_1 = 25 ms when the porosities are less than about 25 percent, and predicted permeability with T_1 =100 ms matches the measured permeability for porosities greater than 25 percent. Note that the cleaner sandstones (C_v < 20 percent) and dirty sandstones (C_v > 20 percent) follow similar trends when water-filled porosities are less than about 25 percent. In figure 6*B*, however, permeability versus water-filled porosities derived from the NE-inversion indicates that the permeability of the clean sandstones follows the predicted permeability with T_1 = 50 ms and that of clay-rich sandstones follows the predicted permeability with T_1 = 12.5 ms for all porosity ranges.

If the water-filled porosity derived from the PS-inversion is more accurate than porosity derived from the NE-inversion, the effect of clay and gas hydrate on permeability appears to be similar. However, if the water-filled porosity derived from the NE-inversion is more accurate, clay has a larger effect on permeability than gas hydrate. The dominant clay type at this well site is illite, and permeability of sandstone with illitic clay is orders of magnitude lower than that of sandstone with kaolinitic clay (Dresser Atlas, 1985). Therefore, the low permeability of clay-rich sandstones near a porosity of 25 percent shown in figure 6*B* is plausible, and porosities estimated from the NE-inversion appear to be more accurate. However, it is not possible to determine which water-filled porosity is more accurate based on permeability, partly because relative permeability is derived from NMR log measurements.

Errors associated with R_w Estimation from NMR Log

Errors associated with the estimated resistivity of connate water using equation 22 with porosity estimated from the NMR or NE-inversion can be written as

$$\frac{\Delta R_w}{R_w} = \frac{\Delta R_t}{R_t} + \frac{m\Delta\phi_{NMR}}{\phi_{NMR}} - \frac{\Delta a}{a} + \frac{\ln(\phi_{NMR})m\Delta m}{m} \qquad (23)$$

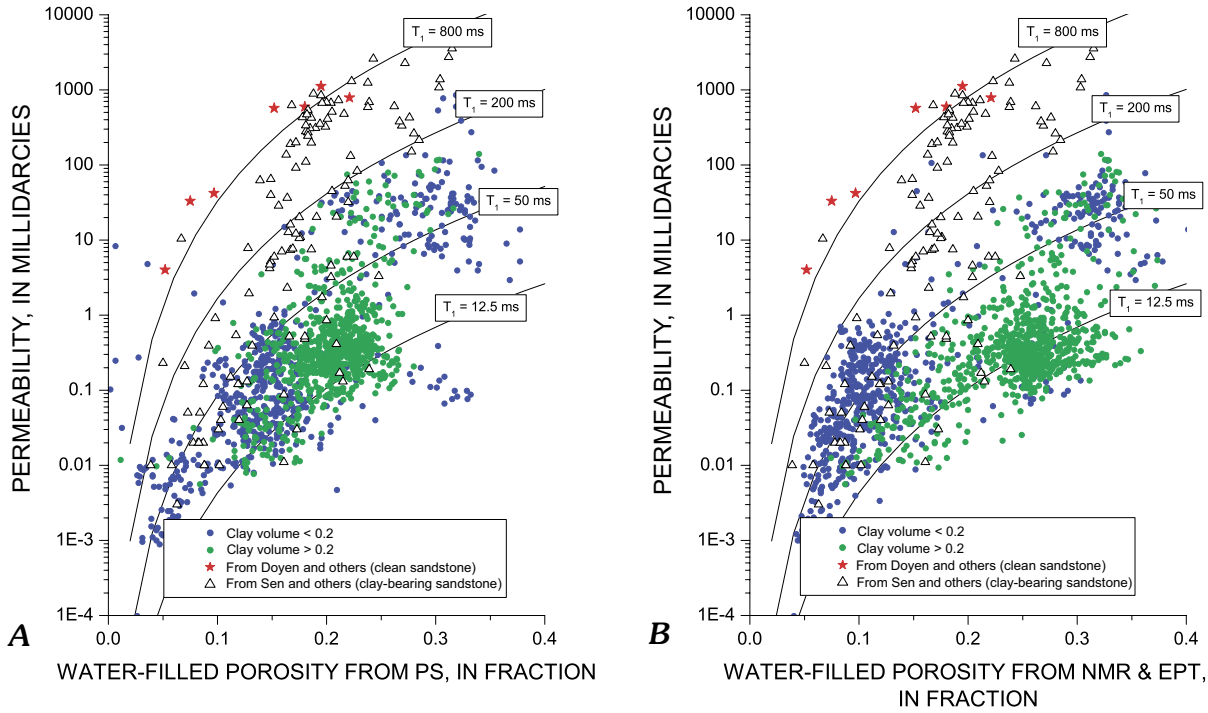

Figure 6. Relationship between permeability and water-filled porosity for samples within gas-hydrate stability zone (891–1,109 m). Measurements are classified into two groups based on clay volume content. *A*, Water-filled porosity calculated from PS-inversion (*P*- and *S*-wave velocity). *B*, Water-filled porosity calculated from NE-inversion (NMR and EPT). Solid and dotted lines represent predicted permeabilities from the empirical relationship by Sen and others (1990). For comparison, permeabilities of clean sandstones measured by Doyen and others (1988) are shown as stars and permeability of clay-bearing sandstones measured by Sen and others (1990) are shown as triangles. NMR, nuclear magnetic resonance; EPT, electromagnetic propagation tool.

For given Archie parameters a and m, the error in the resistivity of connate water depends on the measurement errors in the formation resistivity and NMR porosity. For high gas-hydrate saturations, R_t is large and ϕ_{NMR} is small. Therefore, ΔR_w is dominated by $\Delta\phi_{NMR}$. For example, let us assume that S = 80 percent for a sediment with ϕ = 35 percent. Then, ϕ_{NMR} = (1–0.8) × 0.35 = 0.07. If there is about ±3 percent error in the NMR porosity, $\Delta R_w / R_w = \pm 2.15 \times 0.03/0.07 = \pm 0.92$, or 92 percent error in R_w due to the 3 percent uncertainty in the NMR porosity. On the other hand, at low saturations, the error is much smaller. Let us assume that S = 20 percent, then ϕ_{NMR} = (1–0.2)*0.35 = 0.28. Therefore, $\Delta R_w / R_w = \pm 2.15 \times 0.03/0.28 = \pm 0.23$, or 23 percent error in R_w. This analysis suggests that R_w estimated from the NMR porosity using equation 17 contains a large uncertainty at high gas-hydrate saturations and is more reliable at low saturations.

Estimation of Resistivity of Connate Water, R_w

The electrical resistivity of gas-hydrate-bearing sediments depends on the resistivity of connate water as well as the amounts of gas hydrate. The estimated amounts of gas hydrate depend on the value of R_w used in the estimation. If the estimated R_w is close to the actual in-situ R_w, the estimation is reliable. As mentioned previously, the resistivity of connate water can be derived either from the NMR porosity or porosities derived from NE-inversion or PSR-inversion with a coupling constant.

Figure 7 shows the estimated resistivity of connate water from NE-inversion and PSR-inversion using the Humble equation (that is, a = 0.62 and m = 2.15) (Winsauer, 1952) and computed resistivity using Arp's formula (1953) with measured salinities and temperatures. Figure 7*A* indicates that the agreement between the two estimated resistivities is poor except at depths greater than 1,100 m. Particularly, the estimated R_w using the NE-inversion are higher than measured R_w for the depth interval 1,000–1,075 m, where gas-hydrate saturations estimated from the PSR-inversion are higher than those from the NE-inversion (fig. 2). Figure 7*B* shows that R_w estimated from the PSR-inversion with a coupling constant of 0.1 agrees well with the calculated R_w using salinity and temperature.

Comparing saturations shown in figure 2 and R_w shown in figure 7, it is concluded that R_w from the NE-inversion generally underestimates R_w for high gas-hydrate saturations and overestimates R_w for low gas-hydrate saturations except for depths greater than 1,100 m. As shown previously, for high

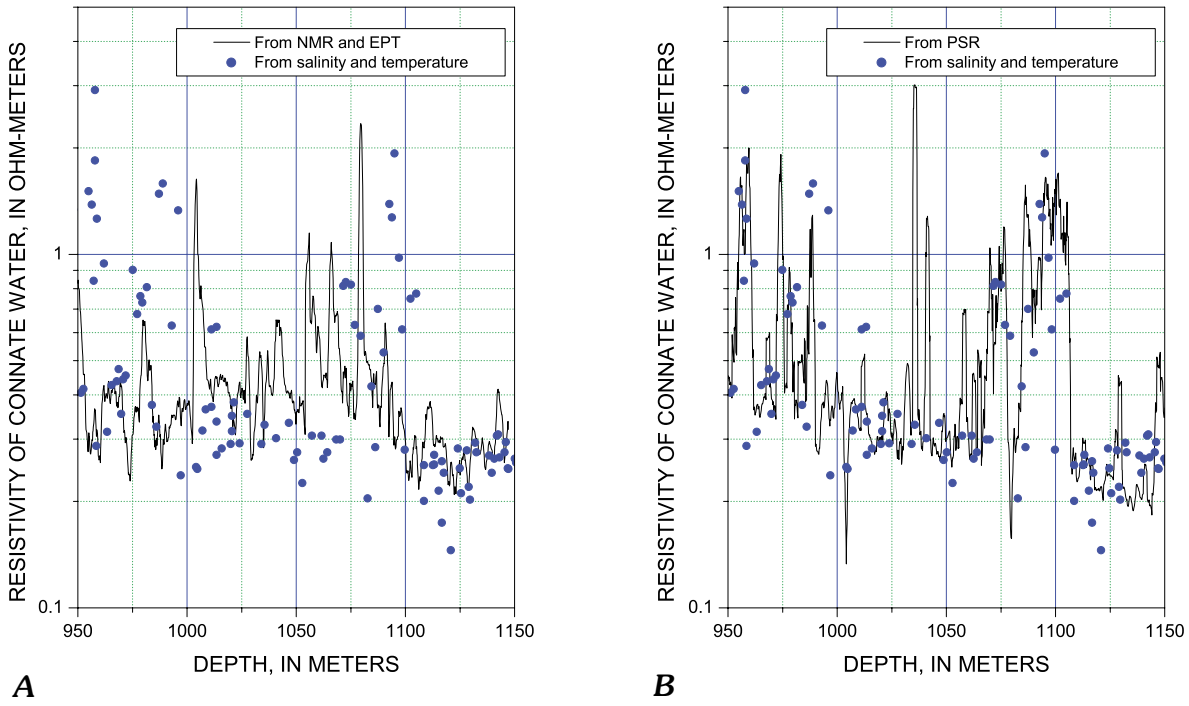

Figure 7. Resistivity of connate water estimated from *A*, NE-inversion (NMR and EPT) and *B*, PSR-inversion using a coupling constant of 0.1 (*P*-wave velocity, *S*-wave velocity, and electrical resistivity). Calculated resistivities of connate water from measured salinity and temperature using Arp's formula (1953) shown as dots. NMR, nuclear magnetic resonance; EPT, electromagnetic propagation tool.

gas-hydrate saturations, a small error in ϕ_{NMR} yields a large error in R_w. Error analysis indicates that R_w estimated from NE-inversion is more reliable at low gas-hydrate saturations. Therefore, for depths between 1,000 and 1,075 m, where low gas-hydrate saturations are estimated from the NE-inversion, the estimated R_w should be accurate, if the porosity from the NE-inversion is accurate. However, the estimated R_w from the NE-inversion is less accurate than that from the PSR-inversion. Therefore, it is probable that NMR or EPT overestimates porosity at that depth interval.

Below the base of the gas-hydrate stability zone (1,109 m), figure 2 shows that the PSR-inversion technique yields gas-hydrate saturations ranging from 10 percent to 20 percent, whereas the NE-inversion method yields no evidence of gas hydrate. Figure 7 indicates that, in this depth interval, R_w estimated from NE-inversion agrees better with the measured R_w than that estimated from the PSR-inversion. The average value of measured R_w within the clean sandstone interval between 1,110 and 1,140 m is about 0.3 ohm-meter, whereas the estimated R_w from the PSR-inversion is about 0.2 ohm-meter. Therefore, error in the R_w is about $\Delta R_w / R_w = -0.5$. According to Lee and Collett (2001b), the error in the gas-hydrate saturations due to $\Delta R_w / R_w = -0.5$ is about 0.2 at zero gas-hydrate saturation. Therefore, the gas-hydrate saturations estimated from the PSR-inversion at depths between 1,110 and 1,140 m are erroneous. This suggests that the overestimation of gas-hydrate saturations comes from the fact that the sediments at depths between 1,130 and 1,140 m would be more consolidated than assumed in the inversion. In other words, $n = 1.1$ used for the inversion is too low for this depth interval. It is emphasized that, in the PSR-inversion, the effect of differential pressure depending on depth is included, but the degree of consolidation remains constant throughout the depth interval. Choosing adjustable parameters accurately is one of the problems in using elastic velocities to estimate gas-hydrate saturations.

Gas-Hydrate Saturations

Gas-hydrate saturations estimated in this paper are based on indirect indications of gas-hydrate-bearing sediments (for example, electrical resistivity, water-filled porosity, and others). Because there is no independent source of gas-hydrate saturations from the Mallik 5L-38, it is difficult to assess the accuracy of each estimation method. Note that all recovered cores experienced some degree of gas-hydrate dissociation, so gas-hydrate saturations estimated from the core are not accurate either (Collett and others, 1999). Therefore, the following discussions focus mainly on the internal consistency of each estimation method.

The advantages of using the NMR or EPT measurement in estimating water-filled porosities or gas-hydrate saturations is that there are no adjustable parameters and the measurements are isotropic. As shown in equation 14, the element of the matrix relating the measurement to unknown variables consists only of the intrinsic properties of the sediment (for example, densities of matrix), pore fluid, and gas hydrate. Therefore, NMR and EPT logs, in theory, provide unbiased estimates of gas-hydrate saturations.

On the other hand, gas-hydrate saturations estimated from elastic velocities and electrical resistivities depend on many adjustable parameters, models, and directions of measurements. For example, the cementation factor m with the resistivity method and the exponent n used in the BGTL are adjustable parameters and calculated gas-hydrate saturations depend on these parameters. Velocity models, for example, pore-filling or cementation models (Sakai, 2000), and seismic anisotropy (Holbrook, 2001) also complicate the estimation of acoustically derived gas-hydrate saturations. Therefore, gas-hydrate saturations are often biased estimates of true saturations.

One enigma encountered during the data analysis at the Mallik 5L-38 well is the discrepancy between gas-hydrate saturations estimated from the NE-inversion and PSR-inversion for the depth interval between 1,000–1,075 m. Estimations of gas-hydrate saturations from the PS-inversion lower than those from the NE-inversion could be explained on the basis of seismic anisotropy, which is observed at the well site (Plona and others, in press). However, higher gas-hydrate saturations estimated from the PS-inversion is not easily explained. This interval corresponds to low gas-hydrate saturations and a high clay content. Based on permeability measurements, porosities estimated from the NE-inversion appear to be more accurate than those from the PSR-inversion. However, based on R_w, estimates from the PSR-inversion method appear to be more accurate than those from the NE-inversion method.

Based on the population relative to gas-hydrate saturations, it is speculated that the uncertainties of saturations associated with the NE-inversion come from the inaccuracy of measurements, not data analysis. The errors in the estimated R_w suggest that NMR could have overestimated porosities of shaly sandstones and underestimated porosities of clean sandstones at the Mallik 5L-38 well. However, in the PSR-inversion, uncertainties come mainly from data analysis. For example, it is difficult to differentiate velocity increase due to compaction/consolidation from gas-hydrate accumulations. If gas hydrates in the pore space support pressure of overlying sediments, the degree of compaction of gas-hydrate-bearing sediments could be less than that of water-saturated sediments at the same depths. Gas-hydrate saturations estimated from the PSR-inversion under this assumption would be different from those shown in this paper.

Irrespective of log types used in the estimation, the saturations are inaccurate at low saturations because small errors in measurements or parameters have more pronounced effects at low saturations (Lee and Collett, 2001b). However, the issue of estimating low saturations of gas hydrate in shaly sandstones is important because most of marine gas hydrates occur in shaly sandstones with low saturations (Collett and Ladd, 2000). Are the NMR or EPT measurements insensitive to the gas hydrate dispersed in shaly sandstone intervals at low

saturations or are the analyses of acoustic and resistivity methods inaccurate in shaly intervals? Is this due to the differences in the depth of investigation of each tool? Or is the accuracy of estimation at low saturations limited by the measurements themselves? In order to answer these questions and to resolve the differences among various measurements, controlled experiments at in-situ conditions are required.

Conclusions

Combining measurements depending on the bulk volume of gas hydrate with measurements depending on the pore-scale interaction as well as the amount of gas hydrate enables us to infer how gas hydrate deposits in the pore space. The analysis of various well logs acquired in the Mallik 5L-38 well supports the pore-filling characteristic of gas hydrate, particularly in clean sandstone intervals. In clean sandstone intervals with high gas-hydrate saturations, gas-hydrate content estimated from the NMR and EPT measurements are comparable to those from *P*-wave, *S*-wave, and resistivity measurements.

In shaly intervals, gas-hydrate estimates from log measurements that depend on the pore-scale interaction between gas hydrate and host sediments (velocity and resistivity logs) are higher than those estimated from measurements that depend on the bulk volume of gas hydrate (NMR and EPT logs). It is not known whether the discrepancy is caused by imperfect models for NMR or EPT, or by the inaccuracy of measurement, or by choosing incorrect adjustable parameters.

Resistivities of connate water in shaly intervals estimated from the PSR-inversion technique compare favorably with water resistivities calculated from direct salinity and temperature measurements, whereas NMR and EPT logs overestimate the resistivity. However, this does not substantiate the notion that the PSR-inversion method provides a more accurate estimation than the NE-inversion method. Without knowing the behavior of NMR and EPT logs in shaly intervals with low gas-hydrate saturations, or the elastic, electric, and properties of gas-hydrate-bearing sediments under controlled conditions, it is difficult to determine which measurement yields more accurate gas-hydrate saturations. Additionally, in shaly intervals, the interaction between gas hydrate and porous media is poorly understood.

References

Akihisa, K., Tezuka, K., Senoh, O., and Uchida, T., 2002, Well log evaluation of gas hydrate saturation in the MITI Nankai Trough well, offshore southeast Japan: SPWLA 43rd Annual Logging Symposium, June 2–5, 14 p.

Archie, C.E., 1942, The electrical resistivity log as an aid in determining some reservoir characteristics: Journal of Petroleum Technology, v. 146, p. 1–8.

Arp, J.J., 1953, The effect of temperature on the density and electrical resistivity of sodium chloride solutions: Petroleum Transaction, American Institute of Mining, Metallurgical, and Petroleum Engineers, v. 198, p. 327–330.

Berg, R.R., 1970, Method of determining permeability from reservoir rock properties: Transactions, Gulf Coast Association of Geological Societies, v. 200, p. 303–317.

Collett, T.S., 1998, Well log evaluation of gas hydrate saturations: Transactions of the 39th Annual Symposium of the Society of Professional Well Log Analysts, Paper MM, unpaginated.

Collett, T.S., 2002, Energy resources potential of natural gas hydrates: American Association of Petroleum Geologists Bulletin, v. 86, p. 1971–1992.

Collett, T.S., and Ladd, J., 2000, Detection of gas hydrate with downhole logs and assessment of gas hydrate concentrations (saturations) and gas volumes on the Blake Ridge with electrical resistivity log data, *in* Paull, C.K. and others, eds., Proceedings of the Ocean Drilling Program, scientific results, v. 164, p. 179–191.

Collett, T.S., Lewis, R. ., Dallimore, S.R., Lee, M.W., Mroz, T.H., and Uchida, T., 1999, Detailed evaluation of gas hydrate reservoir properties using JAPEX/JNOC/GSC Mallik 2L-38 gas hydrate research well downhole well-log displays, *in* Dallimore, S.R. and others, eds., Scientific Results from JAPEX/JNOC/GSC Mallik 2L-38 gas hydrate research well, Mackenzie Delta, Northwest Territories, Canada: Geological Survey of Canada Bulletin 544, p. 295–311.

Dallimore, S.R., and Collett, T.S., 1997, Gas hydrate associated with deep permafrost in the Mackenzie Delta, N.W.T., Canada—Regional overview: Proceedings of the 7th International Conference on Permafrost, 10 p.

Doyen, P.M., 1988, Permeability, conductivity, and pore geometry of sandstone: Journal of Geophysical Research, v. 93, p. 7729–7740.

Dresser Atlas, 1985, A guide to formation damage prevention in fine grained sandstones: Dresser Atlas Industries, Inc., Report, 10/85–9531.

Dvorkin, Jack, and Nur, A., 1996, Elasticity of high-porosity sandstones: Theory for two North Sea data sets: Geophysics, v. 61, p. 1363–1370.

Ecker, Christine, Lumlet, D., Dvorkin, J., and Nur, A., 1998, Sediments within gas hydrates—Internal structure from seismic AVO: Geophysics, v. 63, p. 1659–1669.

Guerin, Gilles, Goldberg, D., and Melster, A., 1999, Characterization of in situ elastic properties of gas-hydrate-bearing sediments on the Blake Ridge: Journal of Geophysical Research, v. 104, p. 17781–17795.

Hearst, J.R., Nelson, P.H., and Paillett, F.L., 2000, Well logging for physical properties: New York, John Wiley & Sons, 483 p.

Helgerud, M.B., 2001, Wave speeds in gas hydrate and sediments containing gas hydrate—A laboratory and modeling study: Palo Alto, Stanford University, Ph.D. dissertation, 249 p.

Helgerud, M.B., Dvorkin, J., Nur, A., Sakai, A., and Collett, T.S., 1999, Elastic-wave velocity in marine sediments with gas hydrates—Effective medium modeling: Geophysical Research Letters, v. 26, p. 2021–2024.

Hill, R, 1952, The elastic behavior of crystalline aggregates: Proceedings of the Physical Society, London, v. A65, p. 349–354.

Holbrook, W.S., 2001, Seismic studies of the Blake Ridge: Implications for hydrate distribution, methane expulsion, and free gas dynamics, *in* Paul, C.K., and Dillon, W.P., eds., Natural gas hydrate—Occurrence, distribution, and detection: Geophysical Monograph Series, American Geophysical Union, no. 124, p. 235–256.

Hyndman, R.D., Yuan, T., and Moran, K., 1999, The saturation of deep sea gas hydrates from downhole electrical resistivity logs and laboratory data: Earth and Planetary Science Letters, v. 172, p. 167–177.

Katz, A.J., and Thompson, A.H., 1986, Quantitative prediction of permeability in porous rock: Physical Review B, v. 34, p. 8179–8181.

Keynon, W.E., 1992. Nuclear magnetic resonance as a petrophysical measurement: Nuclear Geophysics, v. 6, p. 153–171.

Kleinberg, R.L., Flaum, C., and Collett, T.S., in press, Magnetic resonance log of JAPEX/JNOC/GSC and others Mallik 5L-38 gas hydrate production research well: Saturation, growth habit, relative permeability, *in* Dallimore, S.R., and Collett, T.S., eds., Scientific results from the Mallik 2002 Gas Hydrate Production Research Well Program, Mackenzie Delta, Northwest Territories, Canada: Geological Survey of Canada, Bulletin 585.

Kleinberg, R.L., Flaum, C., Griffin, D.D., Brewer, P.G., Malby, G.E., Peltzer, E.T., and Yesinowski, J.P., 2003, Deep sea NMR—Methane hydrate growth habit in porous media and its relation to permeability, deposit accumulation, and submarine slope stability: Journal of Geophysical Research, v. 108, no. B10, 2508, doi:10.1029/2003JB002389.

Krumbein, W.C. and Monk, G.D., 1943, Permeability as a function of size parameters of unconsolidated sand: Transactions of the American Institute of Mining and Metallurgical Engineers, v. 151, p. 153–163.

Lee, M.W., 2002a, Biot-Gassmann theory for velocities of gas-hydrate-bearing sediments: Geophysics, v. 67, p. 1711–1719.

Lee, M.W., 2002b, Joint inversion of acoustic and resistivity data for the estimation of gas hydrate saturation: U.S. Geological Survey Bulletin 2190, 11 p., available at URL <http://geology.cr.usgs.gov/pub/bulletin/b2190/>, accessed May 4, 2005.

Lee, M.W., 2003, Elastic properties of overpressured and unconsolidated sediments: U.S. Geological Survey Bulletin 2214, 10 p., available at URL <http://geology.cr.usgs.gov/pub/bulletins/b2214/>, accessed May 4, 2005.

Lee, M.W., 2005, Well-log analysis to assist the interpretation of 3-D seismic data at Milne Point, North Slope of Alaska: U.S. Geological Survey Scientific Investigations Report 2005-5048, 18 p., available at URL <http://pubs.usgs.gov/sir/2005/5048/>.

Lee, M.W., and Collett, T.S., 1999, Gas hydrate amount estimated from compressional- and shear-wave velocities at the JAPEX/JNOC/GSC Mallik 2L-38 gas hydrate research well, *in* Dallimore, S.R., and others, eds., Scientific Results from APEX/JNOC/GSC Mallik 2L-38 gas hydrate research well, Mackenzie Delta, Northwest Territories, Canada: Geological Survey of Canada Bulletin 544, p. 313–322.

Lee, M.W., and Collett, T.S., 2001a, Elastic properties of gas hydrate-bearing sediments: Geophysics, v. 66, p. 763–771.

Lee, M.W., and Collett, T.S., 2001b, Gas hydrate estimation error associated with uncertainties of measurements and parameters: U.S. Geological Survey Bulletin 2182, 8 p., available at URL <http://geology.cr.usgs.gov/pub/bulletins/b2182/>, accessed May 4, 2005.

Lewis, R.E., and Collett, T.S., in press, JAPEX/JNOC/GSC and others Mallik 5L-38 gas hydrate research well downhole well log and core montages, *in* Dallimore, S.R., and Collett, T.S., eds., Scientific results from the Mallik 2002 Gas Hydrate Production Research Well Program, Mackenzie Delta, Northwest Territories, Canada: Geological Survey of Canada, Bulletin 585.

Nelson, P.H., 1994, Permeability-porosity relationships in sedimentary rocks: Log Analyst, p. 38–62.

Pearson, C.F., Halleck, P.M., Hermes, P.L., and Mathews, M., 1983, Natural gas hydrate deposit: A review of in-situ properties: Journal of Physical Chemistry, v. 87, p. 4180–4185.

Plona, T.J., and Kane, M.R., in press, Anisotropic stress analysis from downhole acoustic logs in the JAPEX/JNOC/GSC and others Mallik 5L-38 gas hydrate production research well, *in* Dallimore, S.R., and Collett, T.S., eds., Scientific results from the Mallik 2002 Gas Hydrate Production Research Well Program, Mackenzie Delta, Northwest Territories, Canada: Geological Survey of Canada, Bulletin 585.

Sakai, A., 2000, Can we estimate the amount of gas hydrates by seismic method?, *in* Sloan and others, eds., Gas hydrates—Challenges for the future: Annals of The New York Academy of Science, v. 715, p. 492–494.

Sen, P.N., Straley, C., Kenyon, W.E., and Whittingham, M.S., 1990, Surface-to-volume ratio, charge density, nuclear magnetic relaxation, and permeability in clay-bearing sandstones: Geophysics, v. 55, p. 61–69.

Sloan, E.D., Jr., 1998, Clathrate hydrates of natural gases: New York, Mercel Dekker, 705 p.

Sun, Yue-Feng, and Goldberg, D., in press, Analysis of electromagnetic propagation tool response in hydrate-bearing formation, *in* Dallimore, S.R., and Collett, T.S., eds., Scientific results from the Mallik 2002 Gas Hydrate Production Research Well Program, Mackenzie Delta, Northwest Territories, Canada: Geological Survey of Canada, Bulletin 585.

Timur, Aytekin, 1968, An investigation of permeability, porosity, and residual water saturation relationships for sandstone reservoirs: The Log Analyst, v. 9, p. 8–17.

Walsh, J.B., and Brace, W.F., 1984, The effect of pressure on porosity and the transport properties of rock: Journal of Geophysical Research, v. 89, p. 9425–9431.

Winsauer, W.O., Shearin, H.M., Jr., Masson, P.H., and Williams, M., 1952, Resistivity of brine-saturated sands in relation to pore geometry: American Association of Petroleum Geologists Bulletin, v. 36, p. 253–277.

Published in the Central Region, Denver, Colorado
Manuscript approved for publication June 28, 2005
Editing, page layout, photocomposition—Richard W. Scott, Jr.
Graphics by the authors